Electronic Supplementary Material (ESI) for Physical Chemistry Chemical Physics.

Supplementary Information: How does Ytterbium chloride interact with DMPC bilayers? A computational and experimental study

Miguel A. Gonzalez[a],* Hanna Barriga[a], Joanna L. Richens[b], Robert V. Law[a], Paul O'Shea[c], and Fernando Bresme[a]

[a] *Department of Chemistry, Imperial College London, London SW7 2AZ, United Kingdom*

[b] *School of Life Sciences, University of Nottingham, Nottingham, United Kingdom and*

[c] *Faculty of Pharmaceutical Sciences, University of British Columbia, Vancouver, Canada*

(Dated: March 10, 2017)

* m.gonzalez12@imperial.ac.uk

I. MOLECULAR DYNAMICS SIMULATIONS

A. Simulation Details

We have carried out molecular dynamics simulations using the GROMACS v.4.5 package. [1] The velocity rescaling thermostat [2] (with relaxation time $\tau_T = 0.2$ ps) and the Parrinello-Rahman semi-isotropic barostat [3] (with relaxation time $\tau_p = 1.5$ ps) were used to perform simulations in the NpT ensemble, at 323 K and 1 bar. Long-range electrostatic interactions were treated using the 2D version of the Particle Mesh Ewald method. [4, 5] We used a direct space cutoff of 1.0 nm for the real part of the Ewald summation and a Fourier spacing of 0.15 nm. For the Lennard-Jones interactions we used a cutoff of 1.6 nm. All the bonds in the lipid molecules were constrained by applying the LINCS [6] algorithm, while the SETTLE [7] algorithm was used to constrain the bonds of the water molecules.

The computations reported in this work focus on systems consisting of one DMPC bilayer, water and $YbCl_3$. We considered two systems. One containing $YbCl_3$ at both sides of the membrane, and another where the salt was added to one side of the membrane only (see Fig.1), in order to mimic conditions similar to those present in our experiments with vesicles. A typical system consisted of 400 DMPC lipids and $\sim$ 56000 molecules of water. The area of the bilayer was large enough to allow cation adsorption and to also the possible nucleation of nanopores. As noted in the main text we did not observe pore nucleation in any of our simulations. The initial configuration for the DMPC bilayer was created by replicating a configuration downloaded from the lipid data base [8]. We replicated the configuration four times on x-y plane.

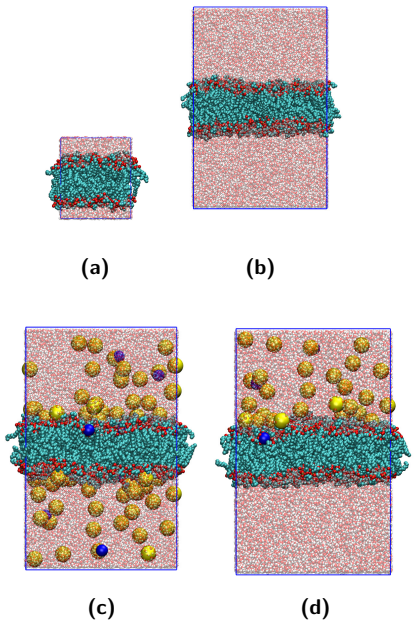

FIG. 1. Snapshots showing the systems simulated in this work. a) Initial configuration from ref. 8 consisting of 100 DMPC lipid. b) System with 400 DMPC and confining walls (not shown) in the upper and lower part. c) System A with 400 DMPC and 10 $YbCl_3$ on both side of the bilayer and confining walls. d) System B with 400 DMPC and 10 $YbCl_3$ on one side of the bilayer, and confining walls. The yellow spheres represent the Cl_-, the blue spheres correspond to Yb^{3+}. The lipids are represented by small green and red spheres.

The main difference between the systems simulated in this work is the symmetry/asymmetry of the salt concentration across the membrane. The symmetric system, System A or $YbCl_3$/DMPC/$YbCl_3$, consisted of 400 DMPC, 20 $YbCl_3$ (10 molecules per leaflet), and *circa* 56000 water molecules. The salt was present on both sides of the bilayer. This system was used to investigate the main properties of the membrane and the influence of the Ytterbium Chloride on the bilayer structure. The second system, System B or $YbCl_3$/DMPC/H_2O, was set up by adding salt (10 $YbCl_3$) on one side of the membrane. We used two different ion concentrations for the asymmetric system (System B). One corresponds to the experimental concentration employed in the NMR studies, 0.025 Yb^{3+}:lipid ratio, and the second concentration was set to 0.25 Yb^{3+}:lipid ratio in order to reproduce conditions corresponding to membranes fully

saturated with salt.

B. Confining walls

We confined the bilayer-solution system between structureless walls to enable the simulation of the asymmetric charge distributions. This setup allowed us to assess the impact of the periodic boundary effects, associated to bilayer-bilayer interactions and the use of full 3D-Ewald. We found that the differences between the 2D approach employed here and full 3D case are small, validating the use of full 3D-Ewald for symmetric systems. We note that other implementations have been proposed, which involve the replication of bilayers or surrounding the aqueous region of the upper and lower leaflets of the bilayer by vacuum regions [9, 10]. All those methods maintain, independently, the water confined in both sides of the membrane.

The confining walls were located at the edges of the simulation box, $z = 0$ and at $z = L_z$, for standard systems. These walls ensure that the salt concentration on both sides of the bilayer is the same. The water/ions-wall interactions were calculated using a Lennard-Jones (9-3) potential with parameters corresponding to an atomic density of 110 nm^3/nm^2. These parameters replicate the bulk density of SPC/E water. The wall interactions act on the oxygen sites of the water molecules, only. The water slab above and below the bilayer leaflets was ~ 6 nm thick, in order to ensure the wall does not influence the bilayer structure.

Because the introduction of a wall into the simulation involves a new interface, this influences indirectly the tension of the bilayer when using the NpT ensemble. We set the global surface tension to zero. An analysis of the pressure tensor profile in our box reveals that the membranes are under a slight tension ~ 10 mN/m which should have a small impact on the properties investigated in this work (see Ref. [11])

C. Computational Methods

We have characterised the structure of the bilayer by computing the area per lipid, the bilayer thickness, the interdigitation coefficient and the area compressibility modulus.

The area per lipid was calculated using the GridMAT-MD [12] code based on the Voronoi tessellation method. The algorithm was applied independently on each leaflet. Although, more rigorous methods exist [11], the method employed here has been shown to predict areas per lipid compatible with the "real" ones, for bilayers with cross sectional areas similar to those employed here. The bilayer thickness was obtained by calculating the average distance between the phosphorous atoms at the two leaflets.

The area compressibility modulus, K_A, can be obtained from the analysis of the area fluctuations of the bilayer,

$$K_A = A\left(\frac{\partial\gamma}{\partial A}\right)_T = \frac{k_B T A}{\langle A^2\rangle - \langle A\rangle^2}, \tag{1}$$

where A is the average area of the simulation box in the plane x-y, γ is the surface tension, k_B is the Boltzmann's constant and T the temperature. We employed the Parrinello-Rahman barostat and a small bilayer area as recommended in Ref. 11. By simulating at these conditions, we obtain results in good agreement with experiments [13] and previous computational studies of PC lipids. [11, 14] The simulations to compute K_A were preformed with a system having two bilayers as indicated in Ref. 9.

The interdigitation coefficient quantifies the degree of overlap of the lipid chains in different leaflets. We employed the method introduced by Das et al. [15]. This approach relies on the calculation of the overlap density, $\rho_{ov}(z)$, of the lipid chains. The overlap is calculated from the densities of each individual leaflet where $\rho_t(z)$ and $\rho_b(z)$ are the density of the tails in the top and bottom layers, respectively. The overlap density is then obtained from,

$$\rho_{ov}(z) = 4\frac{\rho_t(z)\times\rho_b(z)}{[\rho_t(z)+\rho_b(z)]^2} \tag{2}$$

The coefficient of interdigitation is obtained by integrating $\rho_{ov}(z)$ over z,

$$\lambda_{id} = \int_0^{L_z} \rho_{ov}(z)dz, \tag{3}$$

where L_z is the length of the z side box. λ_{id} is equal to zero when there is no overlap between the hydrocarbon chains of lipids located in different leaflets, and equal to one when there is full overlap or interdigitation.

We also quantified the degree of order of the aliphatic chains by computing the order parameter, S_{CD} [16]. S_{CD} measures the alignment of the bond with the bilayer normal.

$$S_{CD} = \frac{1}{2}(3\left\langle \cos^2\theta \right\rangle - 1) \tag{4}$$

where θ is the angle between the bond vector and the membrane normal, z.

II. MATERIALS AND EXPERIMENTAL METHODS

To experimentally verify the computational results, we have studied the interaction of Yb^{3+} and Dy^{3+} ions with extruded dimyristoylphosphatidycholine (DMPC) vesicles using Magic Angle Spinning (MAS) solid state ^{1}H-NMR and fluorescence titration experiments. ^{1}H-NMR has been used to measure chemical shift variations and quenching of the lipid headgroup signal from the external addition of lanthanides (Yb^{3+}, Dy^{3+}) to extruded DMPC vesicles. The fluorescence titration experiments utilise a pre-established assay [17] where lipid vesicles doped with fluoresce in phosphatidylethanolamine (FPE) use fluorescence to quantify equilibrium changes in membrane surface charge from the titration of lanthanides into DMPC lipid vesicles. These two complementary techniques quantify significantly different lipid and lanthanide interactions, however, the data shows similar trends in behaviour with temperature and increasing lanthanide concentration thereby supporting the computational data.

A. Vesicle Preparation

Dimyristoylphosphatidycholine (DMPC) was purchased from Avanti Polar lipids (AL, USA) as a lyophilised powder. The lipids had a purity of >98% and were used without further purification, but were lyophilised for 12 hours before use. Lipids were hydrated to a concentration of 13 mM in 10 mM TRIS, pH 7.4 purchased from Sigma Aldrich (Gillingham, UK) for the fluorescence experiments and 30 mM in D_2O for the MAS-^{1}H NMR experiments. After hydration each sample was heat cycled (between approximately 73 K and 333K) a minimum of 5 times. Lipids were extruded through a 100 nm polycarbonate filter using an Avanti Mini Extruder to form small unilamellar vesicles (SUVs). The different concentrations were used to optimise signal and stability in the two experimental set ups.

Subsequently 15 μL of a 2 mg/ml fluoresce in phosphatidylethanolamine (FPE) chloroform solution was dried under a stream of nitrogen gas followed by resolvation with 15 μl of 95% ethanol. 1 ml of the extruded vesicle solution was added and the mixture was incubated at 310K in the dark for 1.5 h. Unincorporated FPE was then removed via passage through a size exclusion PD-10 Sephadex column purchased from Sigma Aldrich (Gillingham, UK). Samples were stored in an incubator and used within 24 hours. Lanthanides (Ytterbium (III) chloride and Dysprosium (III) chloride) were purchased from STREM Chemicals (Newbury Port, USA) and diluted in 10 mM TRIS, pH 7.4 to 6.5 mM. FPE labelled, extruded vesicle samples were diluted to 400 μM in 10 mM TRIS, pH 7.4 and incubated at the required temperature for a minimum of 15 minutes prior to the experiment. Samples were excited at 490 nm with the emission at 518 nm and collected using a Fluoro log-3 Spectrofluorimeter (HORIBA Jobin Yvon). Lanthanides were titrated into the labelled vesicle solution in sequential volumes, to give a minimum of 10 measurements prior to signal saturation.

B. Titration Assay

Prior to titration experiments a stable fluorescence baseline was achieved by allowing the sample to equilibrate for 10 minutes. Fluorescence changes versus time were measured following serial additions of lanthanide solutions to FPE-labelled SUVs. Following additions, samples were allowed to equilibrate for a minimum of 1 minute and prior to each new titration, equilibrium was achieved. Each experiment was performed using three independently prepared samples at 298, 310 and 321K. Experimental controls comprised subtraction of the fluorescence signal obtained for the appropriate 10 mM TRIS buffer controls from that obtained for the corresponding lanthanide addition. Vesicles were monitored by dynamic light scattering both pre and post lanthanide addition, confirming their stability.

C. Pyranine Assay

DMPC was hydrated in 5 mM HEPES, 0.5 mM pyranine, pH 7.5 purchased from Sigma Aldrich (Gillingham, UK) to a lipid concentration of 30 mM and heat cycled between approximately 73K and 333K a minimum of 4 times.

SUVs were then formed via extrusion through a 100 nm polycarbonate filter using an Avanti Mini Extruder. Unencapsulated pyranine dye was removed via passage through a G-50 Sephadex column (medium, GE Healthcare) and elution into 5 mM HEPES, pH 7.5. The sample was further diluted 100μl in 150μl of elution buffer prior to measurement in a Varian Eclipse fluorimeter. An excitation and emission wavelength of 460 and 510 nm were used respectively. A pH gradient was induced via the addition of 1.5 μl of 1M HCl or 1M HCl with 98.4 mM $YbCl_3$. As a control, 1.5μl of pH 7.5 buffer was added to three samples. Data points are the mean and standard deviation of a minimum of nine measurements and three independent samples. The fluorescence was normalised by dividing by the average of the first 20 data points.

D. Titration Data Analysis

Absolute fluorescence was converted to a percentage change in fluorescence to account for sample variability. Control baselines from the titrations of 10 mM TRIS into labelled vesicle solutions were subtracted from each dataset. The equilibrium fluorescence post titration was plotted as a function of lanthanide concentration and fitted using a Hill fit:

$$\% \text{ fluorescence change} = \frac{V_{max} x^n}{k^n + x^n}, \tag{5}$$

where V_{max} is the maximum % fluorescence change achieved, k is the Michaelis constant and n is the number of cooperative sites. To quantify the concentration of lanthanides at which the fluorescence saturated, the saturation point was defined as 0.9 V_{max} and the value of x (i.e. the concentration in μM) calculated from the fit. This concentration was subsequently converted to an absolute number of lanthanide ions and the ratio of half the number of lipid molecules to lanthanides ions at 0.9 V_{max} calculated. The number of lipids is constant throughout the lanthanide additions. Points shown are the mean and standard error of the results from the independent experiments.

E. NMR Methods

Lanthanides (Ytterbium (III) chloride and Dysprosium (III) chloride) were purchased from STREM Chemicals (Newbury Port, USA) and diluted in D_2O to 0.15 M. Spectra were obtained using MAS-^{1}H NMR (3.8 kHz) on a Bruker 600 MHz spectrometer using a 4 mm Zirconia rotor with a Kel-F cap. Samples were measured followed by a subsequent addition of lanthanide solution to the appropriate lipid:lanthanide ratio as detailed. Spectra are shown in the main article. Chemical shifts and quenching of the N-Methyl lipid headgroup MAS-^{1}H NMR signal were calculated in Origin from fits to normalised data. The spectra were normalised to an integrated area of 1 to account for any experimental differences and the N-Methyl lipid headgroup signal was fitted using the Origin software package using a Gaussian model. The chemical shift was defined as the peak centre and the peak area was calculated and compared to the vesicular peak area in the absence of lanthanides, to calculate the percentage reduction in the N-Methyl lipid headgroup signal upon addition of lanthanide ions.

[1] B. Hess, C. Kutzner, D. van der Spoel, and E. Lindahl, J. Chem. Theory Comput., 2008, **4**, 435–447.
[2] G. Bussi, D. Donadio, and M. Parrinello, J. Chem. Phys., 2007, **126**, 14101.
[3] M. Parrinello and A. Rahman, J. Appl. Phys., 1981, **52**, 7182–7190.
[4] T. Darden, D. York, and L. Pedersen, J. Chem. Phys., 1993, **98**(12), 10089.
[5] U. Essmann, L. Perera, M. L. Berkowitz, T. Darden, H. Lee, and L. G. Pedersen, J. Chem. Phys., 1995, **103**, 8577–8593.
[6] B. Hess, J. Chem. Theory Comput., 2008, **4**(1), 116–122.
[7] S. Miyamoto and P. A. Kollman, J. Comput. Chem., 1992, **13**(8), 952–962.
[8] J. Domański, P. J. Stansfeld, M. S. P. Sansom, and O. Beckstein, J. Membr. Biol., 2010, **236**, 255–258.
[9] A. A. Gurtovenko and I. Vattulainen, J. Am. Chem. Soc., 2005, **127**(50), 17570–17571.
[10] L. Delemotte, F. Dehez, W. Treptow, and M. Tarek, J. Phys. Chem. B, 2008, **112**(18), 5547–5550.
[11] E. Chacón, P. Tarazona, and F. Bresme, J. Chem. Phys., 2015, **143**(3), 034706.
[12] W. J. Allen, J. A. Lemkul, and D. R. Bevan, J. Comput. Chem., 2009, **30**(12), 1952–1958.
[13] W. Rawicz, K. C. Olbrich, T. McIntosh, D. Needham, and E. Evans, Biophys. J., 2000, **79**(1), 328–339.
[14] Q. Waheed and O. Edholm, Biophys. J., 2009, **97**(10), 2754–2760.
[15] C. Das, M. G. Noro, and P. D. Olmsted, Biophys. J., 2009, **97**(7), 1941–1951.

[16] L. V. Schäfer, D. H. de Jong, A. Holt, A. J. Rzepiela, A. H. de Vries, B. Poolman, J. A. Killian, and S. J. Marrink, Proc. Natl. Acad. Sci., 2011, **108**(4), 1343–1348.
[17] J. Wall, C. A. Golding, M. V. Veen, and P. O'Shea, Mol. Membr. Biol., 1995, **12**(2), 183–192.